

# A cosmological study of the star formation history in the solar neighbourhood

X. Hernández<sup>1</sup>, Vladimir Avila-Reese<sup>1</sup> and Claudio Firmani<sup>1,2</sup>

<sup>1</sup> Instituto de Astronomía, Universidad Nacional Autónoma de México, A.P. 70-264, 04510 México, D.F.

<sup>2</sup> Osservatorio Astronomico di Brera, via E. Bianchi 46, 23807 Merate (LC), Italy

24 October 2018

## ABSTRACT

We use a cosmological galactic evolutionary approach to model the Milky Way. A detailed treatment of the mass aggregation and dynamical history of the growing dark halo is included, together with a self consistent physical treatment for the star formation processes within the growing galactic disc. This allows us to calculate the temporal evolution of star and gas surface densities at all galactic radii, in particular, the star formation history (SFH) at the solar radius. A large range of cosmological mass aggregation histories (MAHs) is capable of producing a galaxy with the present day properties of the Milky Way. The resulting SFHs for the solar neighbourhood bracket the available observational data for this feature, the most probable MAH yielding the optimal comparison with these observations. We also find that the rotation curve for our Galaxy implies the presence of a constant density core in its dark matter halo.

**Key words:** Cosmology: dark matter — Galaxy: evolution — Galaxy: halo — galaxies: formation — solar neighborhood — stars: formation

## 1 INTRODUCTION

The star formation history (SFH) of galaxies is a key ingredient in describing their evolution. From an observational point of view, the SFH can be studied by measuring the integrated light of the galaxy population as a whole or of a homogeneous sample of galaxies at different redshifts, at wavelengths associated with massive star formation (e.g., Madau, Pozzetti & Dickinson 1998; Lilly et al. 1998). An alternative method, which avoids the difficulties in selecting a homogeneous sample of galaxies, determines the SFH of a specific galaxy using multi-band photometry and chemical abundances combined with population synthesis models. In the case of the Milky Way (MW), the large amount of available data allows to qualitatively constrict the input SFHs of these methods with some accuracy (e.g., Prantzos & Aubert 1995; Chiappini, Matteucci, & Gratton 1997; Carigi 1997; Boissier & Prantzos 1999).

On the same line of multi-band photometry, but with higher precision, the SFH of a system can be obtained through the study of its resolved stellar population. This allows to construct colour-magnitude diagrams, which contain detailed information on the SFH behind such diagrams. Inverting the problem however, is not trivial, with the answer

depending sensitively on the assumed metallicity of the object being studied at every time, i.e., the enrichment history. The accuracy of these inferences being also crucially determined by the depth and error level of the observations, these requirements have so far severely constrained the applicability of such direct inferences to only a handful of astrophysical systems. Still, such methods have recently been applied to systems where the metallicity has been independently determined, and where high quality data exist. Examples being the works of Chiosi et al. (1989), Aparicio et al. (1990) and Mould et al. (1997) using Magellanic and local star clusters, and Mighell & Butcher (1992), Smecker-Hane et al. (1994), Tolstoy & Saha (1996), Aparicio & Gallart (1995), Mighell (1997) and Hernandez et al. (2000a) using local dSph's.

With the coming of high quality photometric data from the Hipparcos satellite, colour magnitude diagram inversion methods using rigorous statistical analysis (Tolstoy & Saha 1996; Hernández et al. 1999 and more references therein) can be applied to the solar neighbourhood SFH. For example, the advanced Bayesian analysis introduced by Hernández et al. (2000b), allows the recovery of the underlying SFH without the need of assuming any *a priori* structure or condition on the SFH. With the Hipparcos catalogue the time resolu-

tion of this technique is  $\sim 0.05$  Gyr, however, the age range which it allows to explore is small (the last 3 Gyr); this limitation is related to the completeness of the Hipparcos solar neighbourhood sample. With a standard parametric maximization technique, Bertelli & Nasi (2001) were able to recover the SFH along the whole life of the solar neighbourhood, at the expense of a low time resolution.

The high quality SFH which can be inferred locally allows the unique opportunity of studying directly the evolution of an individual cosmological object (the Galaxy). This avoids the problems inherent to high redshift studies, such as the uncertainties in relating a population of poorly understood and barely resolved objects to a particular class of present day systems.

Once the SFH of an observed system is known, the goal is to understand its physical evolution. From a theoretical point of view, the challenge is to link the SFH to the structure, dynamics and hydrodynamics of modeled galaxies. Examples of galaxy evolutionary studies in a cosmological context are: White & Frenk (1991), Lacey & Silk (1991), Kauffmann, White & Guiderdoni 1993, Cole et al. (1994), Baugh, Cole & Frenk (1997), van den Bosch (1998), Somerville & Primack (1999), Buchalter, Jiménez & Kamionkowski (2001) and Kauffmann, Charlot & Balogh (2001). A potential shortcoming of many of the above approaches remains the use of somewhat *ad hoc* or empirical schemes for calculating the star formation (SF) in the forming discs.

We improve on this last point by including a physically self consistent scheme of calculating the SF process, where the SF in the disc is induced by gravitational instabilities and is self-regulated by an energy balance in the ISM (Firmani & Tutukov 1992, 1994; Firmani, Hernández, & Gallagher 1996). Combining the above with a cosmological evolutionary approach (Avila-Reese, Firmani & Hernandez 1998 and Firmani & Avila-Reese 2000) yields a powerful tool for exploring the consequences of any particular cosmology in terms of a detailed SFH (Avila-Reese & Firmani 2001).

In this work we make use of this evolutionary approach to infer the SFH of the MW. The cosmological scenario used allows to constrain the SF history of the solar neighbourhood to a narrow range of possibilities, and to identify the most likely of them. Comparison with the available direct observational inferences shows that the local SFH has in fact been very close to the maximum likelihood solution we find. Along similar lines, Hernández & Ferrara (2001) have studied the link between the cosmological build up of the Milky Way and the IMF of population III stars, by analyzing the metallicity distribution of extremely metal poor Galactic halo stars.

In §2 a brief description of the method is presented, emphasizing on the physics of the SF. In §3 we apply this method to model a MW galaxy. The SFH at the solar radius is presented and compared with observations in §4. Section 4.1 is devoted to exploring the sensitivity of the predicted SFH to the input parameters which define our MW model; these parameters were settled from observational constraints which are subject to uncertainties. In the discussion we compare our results with those of chemo-spectrophotometric models (§5.1), and we discuss the possibility of an inter-

mittent SF, as well as other physical mechanisms capable of triggering SF (§5.2). Our conclusions are presented in §6. Throughout this work we assume the currently favored cosmology, a flat universe with non-vanishing vacuum energy ( $\Omega_m = 0.3$ ,  $\Omega_\Lambda = 0.7$ ,  $H_0 = 65 \text{ km s}^{-1} \text{ Mpc}^{-1}$ ,  $\sigma_8 = 0.9$ ).

## 2 THE MODEL

The overall method of disc galaxy evolution used here was presented in Firmani & Avila-Reese (2000, henceforth FA00) and Avila-Reese & Firmani (2000, henceforth AF00) (see also Firmani, Avila-Reese & Hernández 1997). Galactic discs form inside-out within a growing CDM halo, as the baryonic content of the growing halo is incorporated into the disc. The evolution of the halo is set by its mass aggregation history (MAH), determined by an extended Press-Schechter formalism. For a given present-day total virial mass  $M_v$ , a statistical set of MAHs is calculated from the initial Gaussian density fluctuation field once the cosmology and power spectrum are fixed (Lacey & Cole 1993; Avila-Reese et al. 1998). The behaviour of the growth of the halo in mass as a function of redshift can be seen in Fig. 1b, which shows a sample of five realizations of possible MAHs. Fig. 1a gives the average over a statistical sample of  $2 \times 10^4$  Monte Carlo realizations for a  $2.8 \times 10^{12} M_\odot$  halo. Although the “average MAH” clearly smoothes over the discontinuous behaviour of any particular MAH, it provides the simplified version for the most probable mass aggregation process of a large sample of galaxies. Further, the discontinuous behaviour seen in the individual MAHs of Fig. 1b, as reflected in gas accretion, will be naturally smoothed over by the gas virialization and cooling processes in the growing galactic halo.

The density profile of the virialized part of the growing halo is calculated with a generalization of the secondary infall model, based on spherical symmetry and adiabatic invariance, but allowing for non-radial orbits with fixed pericentre to apocentre distance ratios  $\epsilon$  (Avila-Reese et al. 1998). The halo density profile we obtain depends on the MAH and  $\epsilon$ , with the average MAH and  $\epsilon \approx 0.2$  giving density profiles very close to the Navarro, Frenk & White (1997, NFW) profile (Avila-Reese et al. 1998, 1999).

A fraction  $f_d$  of the mass of each collapsing spherical shell is transferred in a virialization time into a central disc gas layer. Assuming angular momentum conservation, a given gas element of the shell falls into the equatorial plane at the position where it reaches centrifugal equilibrium. Each shell is assumed to be initially in solid body rotation, with a specific angular momentum given by:

$$j_{sh}(t) = \lambda \frac{GM_v(t)^{5/2}}{|E(t)|^{1/2}} \left( \frac{5}{2} \frac{1}{M_v(t)} - \frac{d|E(t)|}{2|E(t)|dM_v(t)} \right), \quad (1)$$

where  $E$  is the energy of the halo at time  $t$ , and  $\lambda$  is the halo spin parameter assumed here to be constant in time. The contraction of the dark halo due to the gravitational drag of the infalling gas is calculated within an adiabatic invariance scheme. A nearly exponential disc surface density arises naturally in this inside-out scheme of disc formation (e.g. FA00). The  $\lambda$  parameter determines the scale length

a very robust prediction of the Gaussian initial fluctuation hypothesis within the inflationary CDM cosmology.

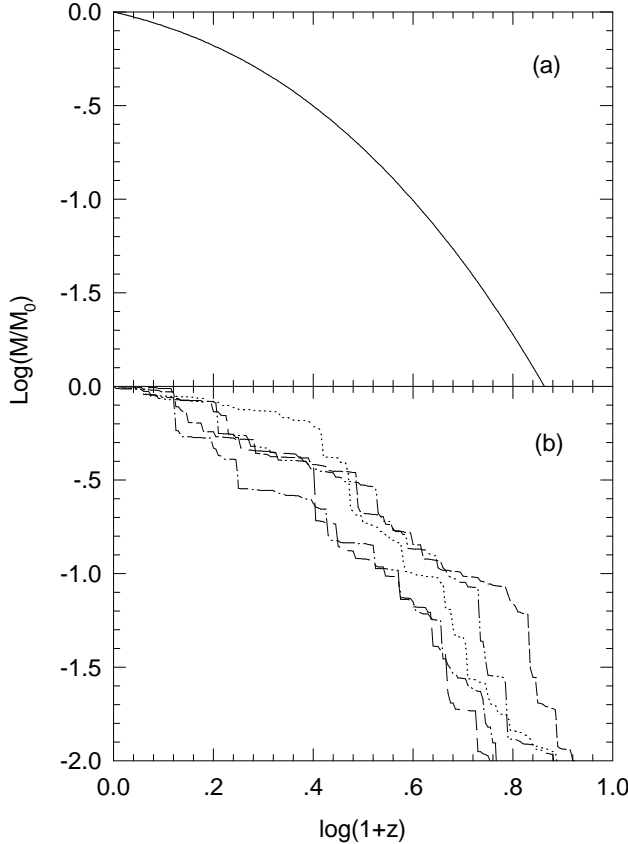


**Figure 1.** a) Average MAH for a galaxy having the present day asymptotic circular velocity,  $V_{50}$ , as the Milky Way. b) Five random realizations of cosmological MAHs yielding the same final asymptotic circular velocity as in a).

and surface density of the disc. According to analytical and numerical studies,  $\lambda$  has a log-normal distribution with an average of  $\sim 0.05$  and a width in the logarithm of less than 1.0 (e.g., Catelan & Theuns 1996 and references therein).

We note that if the dynamical consequences of the MAHs we are using were taken into account, the repeated merging of substructures would destroy the forming discs (Navarro & Steinmetz 2000). This is a shortcoming general to all hierarchical galactic formation models, related to the overabundance of substructure seen at galactic scales (Klypin et al. 1999, Moore et al. 1999a), the excessive mass concentration in the central region of CDM haloes (e.g., Moore 1994, Burkert & Silk 1997, Hernandez & Gilmore 1998), and the loss of angular momentum of the gas during incorporation into the forming galaxy (Navarro & Benz 1991). All these difficulties might indeed imply modifications to the overall standard scenario. At this point we introduce as a working hypothesis the assumption that such modifications might result only in a more gentle and homogeneous mass accretion, without altering the overall structure formation and growth model, which appears at the moment

## 2.1 Disc star formation

As the disc begins to form in the centre of the growing CDM halo, transformation of cold gas into stars takes place whenever Toomre's instability parameter for the gaseous disc,  $Q_g(r) = v_g(r)\kappa(r)/\Sigma_g(r)$ , is less than a given threshold,  $q$  (where  $v_g$  and  $\Sigma_g$  are the gas turbulent rms velocity and surface density, and  $\kappa$  is the epicyclic frequency, Toomre 1964). A fraction of the formed stars explodes as SNe, re-heating the gas disc column and increasing  $Q_g(r)$  above the instability threshold. This inhibits SF temporarily, whilst the gas disc column dissipates its turbulent energy, decreasing  $v_g$  back to the value when  $Q_g(r)$  becomes smaller than  $q$ . Actually we calculate the SF rate (SFR) directly from the equation that relates the energy input with the energy dissipation assuming that  $Q_g(r)$  is always equal to  $q$  at all radii, i.e. we allow only for the stationary solution (a more detailed description can be found in Firmani & Tutukov 1994; Firmani et al. 1996). We also consider heating due to the infalling gas, although its contribution is much smaller than the SN input.

While the SFR is rather insensitive to  $q$ , the gas disc height strongly depends upon it. Numerical and observational studies suggest thresholds of the order of  $q = 2$  (see references in FA00). Further, for  $q = 2$ , we obtain realistic values for the gas disc height of a Milky Way (MW) model at the solar neighbourhood. The turbulent dissipation time  $t_d(r)$  is calculated following a simple approach given in Firmani et al. (1996):

$$t_d = \alpha \frac{\delta r}{v_g} = \alpha \frac{1}{V/r + dV/dr} = \alpha \frac{2\Omega}{\kappa^2} \quad (2)$$

where  $\delta r$  is the mean free radial distance traveled by a turbulent cell at Galactocentric radius  $r$  with a speed  $v_g$  ( $\delta r$  is assumed to be much smaller than the orbital length),  $V$  and  $\Omega$  are the circular and angular velocities, and  $\alpha$  is a parameter close to unity. Estimates of the turbulent dissipation time in the solar neighbourhood obtained in compressible magneto-hydrodynamic simulations of the ISM (Avila-Reese & Vázquez-Semadeni 2001) give a lower limit that is roughly half the time given by Firmani et al. (i.e.  $\alpha \gtrsim 0.5$  in eq. (2)). It should also be taken into account that in the real ISM, besides turbulence, magnetic fields and cosmic rays contribute to the pressure, in such a way that the  $t_d$  found in the turbulence simulations could be only a lower limit to the global energetic dissipation time in the ISM. We shall use here  $\alpha = 0.7$ .

The evolution of the stellar populations is followed with a parameterization of simple population synthesis models (see Firmani & Tutukov 1992, 1994). A Salpeter IMF with minimal and maximal masses of  $0.1M_\odot$  and  $100M_\odot$ , and solar metallicities were used.

The azimuthally averaged dynamics of the evolving gas and stellar discs coupled with the dark halo are treated by solving the corresponding hydrodynamical equations. With our method we obtain the temporal evolution of the gas

infall rate on the disc  $\dot{\Sigma}_g(r, t)$ , the SFR  $\dot{\Sigma}_s(r, t)$ , the disc gas and star surface densities,  $\Sigma_g(r, t)$  and  $\Sigma_s(r, t)$ , and the circular velocities due to the disc and halo,  $V_d(r, t)$  and  $V_h(r, t)$ , respectively at all radii. In our model the halo structure and the disc gas infall rate are directly related to the cosmology.

We find that the local SFR typically follows a Schmidt law,  $\dot{\Sigma}_s(r) \propto \Sigma_g^n$ , with  $n \approx 2$  along a major portion of the disc (Firmani et al. 1996; AF00). This SF law is basically a consequence of the self-regulation mechanism we use. It is important to mention that in our models, self-regulation takes place only *within the disc* and not at the level of a hypothetical intra-halo medium in virial equilibrium with the CDM halo (e.g., White & Frenk 1991; Cole et al. 1994; Baugh et al. 1997; van den Bosch 1998; Somerville & Primack 1999). The ISM of normal disc galaxies is dense and very dissipative. Hence, one expects gas and kinetic energy outflows to be confined mostly near the disc (see numerical results and more references in Avila-Reese & Vázquez-Semadeni 2001). Nonetheless, in some cases and at early epochs, the disc-halo feedback may be important; in our model this ingredient may be taken into account by the free parameter  $f_d$ , at least in a first approximation.

### 3 MODELING THE MILKY WAY

For a given cosmology a model is completely determined by the virial mass  $M_v$ , the MAH, the spin parameter  $\lambda$ , and the disc mass fraction  $f_d$ , as all other parameters are fixed by physical considerations.

In order to calculate a model representative of the MW, we have to correctly chose these input parameters so as to fit the observational constraints. Fortunately, each one of these parameters is tightly related to a given present-day MW feature, although with some (small) degeneracy. Due to this degeneracy and to the observational uncertainties in the MW observational constraints, it is necessary to carry out some “parameter-space” exploration.

The total mass of the MW is amongst the most poorly known of all Galactic parameters. Several estimates give values around  $1.0 - 4.0 \times 10^{12} M_\odot$  (see e.g., Wilkinson & Evans 1999 and more references therein). A more robust quantity is the mass within a certain large radius (50 kpc for example) constrained by the motions of satellite galaxies, globular clusters, the local escape velocity of stars, etc. Using these constraints together with the observed rotation curve of the disc, Kochanek (1996) determined the MW mass within 50 kpc. This mass implies a circular velocity  $V_{50}$  of  $206^{+10}_{-11}$  km s $^{-1}$  ( $206^{+22}_{-25}$  km s $^{-1}$ , at 90% C.L.). A more recent determination of  $V_{50}$  by Wilkinson & Evans (1999), constructed from the current data set of objects (27) with known distances and radial velocities at Galactocentric radii greater than 20 kpc, is consistent with the values found by Kochanek (1996). A  $V_{50}$  of  $206^{+10}_{-11}$  km s $^{-1}$  is the observational constrain we use to fix the virial mass of the MW model for a given MAH. Since the MAH determines the halo density profile,  $M_v$  will be different for different MAHs; for the average MAH, this mass is  $M_v = 2.8 \times 10^{12} M_\odot$ .

**Table 1.** Properties of the MW: observations and model results

Observable	Predicted value <sup>a</sup>	Observed value	Reference
$V_c(50)$ <sup>b</sup> [km s $^{-1}$ ]	208	$206 \pm 10$	1,2
$r_s$ [kpc]	3.0	$3.0 \pm 0.5$	3
$M_s$ <sup>c</sup> [ $10^{10} M_\odot$ ]	4.4	4-5	4,5
$M_v$ [ $10^{12} M_\odot$ ]	2.8	1-4	2,6
$V_{\max}^d$ [km s $^{-1}$ ]	235	$220 \pm 10$	7,8,9,5
$L_B$ [ $10^{10} L_{B_\odot}$ ]	1.7	$1.8 \pm 0.3$	10,9
$r_B$ <sup>e</sup> [kpc]	4.3	4-5	11
$\Sigma_{0,K}$ <sup>f</sup> [ $L_{K\odot} pc^{-2}$ ]	810	$1000 \pm 200$	11
$f_g$	0.23	0.15 – 0.20	12
SFR [ $M_\odot yr^{-1}$ ]	2.9	2-6	13,14
<i>Solar neighborhood</i>			
$\Sigma_s$ [ $M_\odot pc^{-2}$ ]	41.3	$43 \pm 5$ <sup>g</sup>	4
$\Sigma_g$ [ $M_\odot pc^{-2}$ ]	13.6	$13 \pm 3$	15
$\dot{\Sigma}_s$ [ $M_\odot Gyr^{-1} pc^{-2}$ ]	3.1	3-5	16,17
$B - K$ [mag]	3.15	3.13	8

<sup>a</sup> The MW model was obtained tuning three input parameters in order to reproduce the first three quantities, which are constraints and not predictions

<sup>b</sup> Circular (asymptotic) velocity at 50 kpc.

<sup>c</sup> Stellar (disc+bulge) mass.

<sup>d</sup> This maximum rotation velocity  $V_{\max}$  does not take into account the nuclear and bulge region and it is for Galactocentric radii smaller than 15 kpc; the observational determinations at larger radii are uncertain.

<sup>e</sup>  $B$ -band disc scale length.

<sup>f</sup> Disc central surface brightness in the  $K$ -band, taking a mass to light ratio of 1.0 for this band.

<sup>g</sup> This estimate includes the contribution of stellar remnants.

References: 1. Kochanek 1996; 2. Wilkinson & Evans 1999; 3. Sackett 1997; 4. Mera et al. 1998; 5. Dehnen & Binney 1998a; 6. Méndez et al. 1999; 7. Fich & Tremaine 1991; 8. Binney & Merrifield 1998; 9. Binney & Tremaine 1987; 10. van der Kruit 1986; 11. Kent et al. 1991; 12. see BP99; 13. Prantzos & Aubert 1995; 14. Pagel 1997; 15. Kulkarni & Heiles 1987; 16. Talbot 1980 17. Rana 1987

The spin parameter  $\lambda$  mainly influences the stellar disc scale length and the surface density. The stellar scale length  $r_s$  of the MW inferred from observations in infrared bands or estimated from dynamical constraints is typically  $3.0 \pm 0.5$  kpc (Sackett 1997), this becomes our second constraint. However, see for example Drimmel & Spergel 2001 where values even smaller than these were found. For the average MAH, the observed central value of  $r_s$  yields  $\lambda = 0.02$ .

Once  $M_v$  is given,  $f_d \equiv M_d/M_v$  is fixed by the MW disc+bulge mass  $M_d$ . Most baryons are in the disc+bulge system:  $4 - 5 \times 10^{10} M_\odot$  in form of stars ( $M_s$ , our third constraint) and at least  $\sim 0.6 - 1.0 \times 10^{10} M_\odot$  in form of gas ( $M_g$ ) (see Table 1). The estimated masses of the stellar halo ( $\approx 4.6 \times 10^9 M_\odot$ , Haud & Einasto 1989) and of all MW

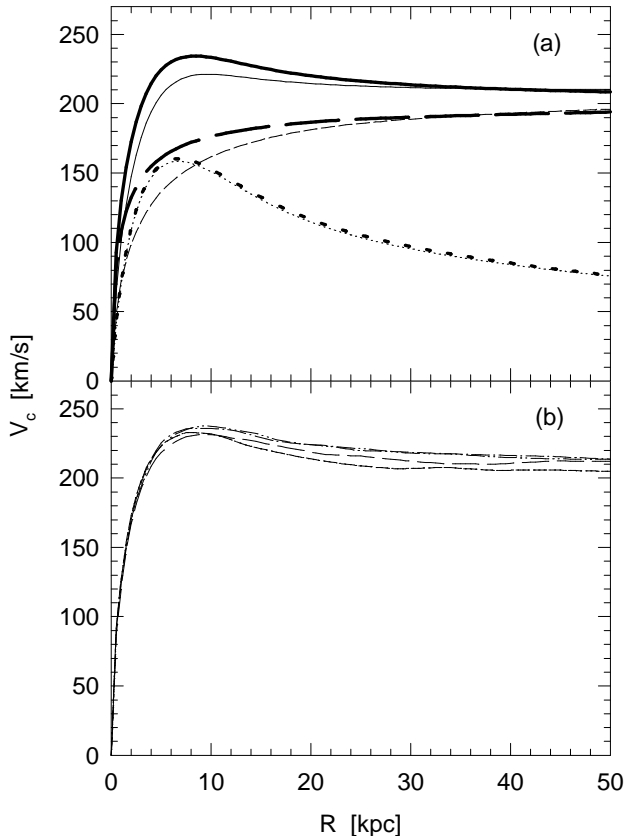


**Figure 2.** a) Rotation curve decomposition for the fiducial Galaxy model giving the total, halo and disc contributions, solid dashed and dotted thick lines, respectively. The thin lines are analogous to the thick ones, showing the case of artificially imposing a 10 kpc constant density core on the dark halo. b) Different final rotation curves, for MW models resulting from the various MAHs shown in Fig. 1b, with line style corresponding to the particular cases of Fig. 1b.

satellite galaxies ( $\sim 6 - 9 \times 10^9 M_\odot$ ) represent only a minor contribution with respect to the disc+bulge system. Taking the average of MAH we obtain  $f_d=0.021$ .

The influence of different MAHs is felt upon the integral galaxy color index, gas fraction  $f_g$ , and scatter in the Tully-Fisher relation. Unfortunately the MAH cannot be described by one-parameter and the color index and gas fraction are not accurately determined for the MW. Thus, we are left with a large range of possible MAHs, all of which lead to models with the same  $V_{50}$ ,  $r_s$  and  $M_s$  for the MW. However, the SFH in the disc of the evolving galaxy, and particularly at the solar radius, is always highly sensitive to the input MAH. The range of MAHs allowed by the structural constraints taken hence defines a range of possible SFHs for the solar neighbourhood, with the most likely being that associated to the average MAH. A comparison with the inferred SFH of the solar neighbourhood, explored in §4, in fact shows the MAH of our Galaxy to have been close to the average one for systems of the MW mass.

The observational estimates of  $V_{50}$ ,  $r_s$  and  $M_s$  given

in Table 1 are thus the constraints we require in order for a model to be considered representative of the MW. For a given MAH the previous conditions allow to determine  $M_v$ ,  $\lambda$  and  $f_d$ . When the average MAH is assumed we obtain  $M_v = 2.8 \times 10^{12} M_\odot$ ,  $\lambda = 0.02$  and  $f_d = 0.021$ . These conditions determine our MW central model, which represents a cosmological maximum likelihood solution, given the structural parameters of our Galaxy (fiducial model).

It should be noted that the values of  $f_d$  and  $\lambda$  used in order to reproduce the stellar mass and scale length of the MW, are smaller than those used in other studies (Dalcanton, Spergel & Summers 1997; Mo, Mao & White 1998; FA00, AF00). The disc mass fraction in haloes,  $f_d$ , used in these works was  $\approx 0.05$ , only slightly smaller than the baryon to total mass fraction,  $\Omega_b/\Omega_m$ , for the conservative value of  $\Omega_b h^2 \approx 0.010$  (Hogan 1998) and  $\Omega_m = 0.3$ . This disc mass fraction increases to  $f_b \approx 0.15$  taking into account the higher estimate of  $\Omega_b h^2$  ( $\approx 0.019$ ) inferred from the deuterium absorption in quasars (Burles et al. 1998). Thus, for the MW the baryon fraction  $(M_d + M_{\text{stellar halo}} + M_{\text{satellites}} + \dots)/M_v$  seems to be smaller than the universal baryon fraction. Cosmological numerical simulations indeed show that most of the baryons in the past and in the present are not within gravitationally bound systems, but in form of diffuse and warm-hot intergalactic gas (Cen & Ostriker 1999; Davé et al. 2000). Smaller values of  $f_d$  allow for smaller values of  $\lambda$  (given a fixed  $r_s$ ) that otherwise could lead the disc to destructive gravitational instabilities (see Mo et al. 1998; FA00). If the distribution of  $\lambda$  is mainly responsible for the galaxy distribution in surface brightness, then, that high-surface brightness MW-type galaxies should have  $\lambda \approx 0.02$  agrees with a distribution where low surface brightness (LSB) galaxies ( $\lambda \gtrsim 0.05$ ) are equally abundant (e.g. McGaugh 1996). To conclude, the values for  $f_d$  and  $\lambda$  inferred for the average MAH seem to be consistent with several observational and theoretical pieces of evidence.

### 3.1 Rotation curve decomposition

In Fig. 2a the rotation curve decomposition of the fiducial MW model is shown by the thick lines, with the continuous curve giving the total rotation curve, the dashed one the halo component, and the dotted one the disc contribution, at the present epoch. The maximum of the final rotation curve occurs at  $\approx 2.2 r_s$  with a value of  $235 \text{ km s}^{-1}$ .

The model rotation curve is somewhat more peaked than the observed one (Fich & Tremaine 1991) and the halo component dominates over the disc component at almost all radii. This is a direct consequence of the high central mass concentration of the CDM halo. There is no way of obtaining a flat rotation curve for the parameters of the MW when a CDM halo is used. The density profile of our ‘virgin’ CDM halo (without the gravitational drag due to disc formation) is well described by the NFW profile. Recent very high-resolution simulations show that the inner density profile of CDM haloes is even steeper than the  $r^{-1}$  slope of NFW profiles (Moore et al. 1999b; see also Fukushige & Makino 1997). The rotation curve of a MW model in this case would be even more peaked than that shown in Fig. 2,

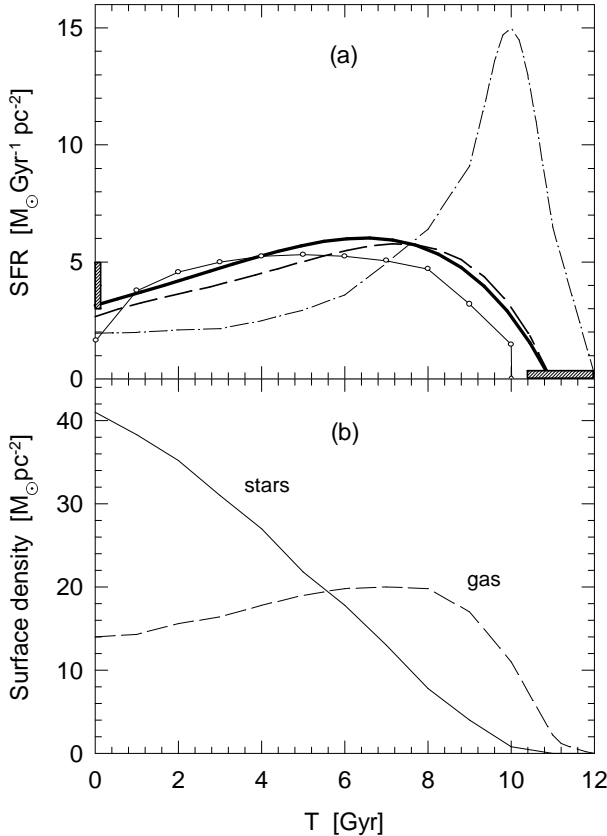


**Figure 3.** a) The thick solid curve gives the predicted SFH for the solar neighbourhood corresponding to the most probable cosmological MAH (the average MAH), with the corresponding gas accretion history at the solar neighbourhood given by the dot-dashed curve. Also shown are the observational inferences of BDB00 for the age of the solar neighbourhood, horizontal shaded box, and of Talbot 1980 and Rana 1987 for the present day value of the SFR, vertical shaded box. The jointed circles give the indicative inferences of Bertelli & Nasi (2001). Our prediction for the average MAH clearly complies with the available observational restrictions for the local SFH. b) This panel shows the evolution of the gas and stars surface densities at the solar neighbourhood, dashed and solid lines, respectively. The present day values being in good accordance with observations.

which should be taken as a lower limit in terms of the central overshooting. The intrinsic scatter in the density profiles of CDM haloes does not help to alleviate this problem, as can be seen in Fig. 2b, where the total final rotation curves corresponding to the five particular MAHs of Fig. 1b are shown.

Several pieces of evidence point out that dark matter haloes at all scales indeed have constant density cores (Moore 1994, Flores & Primack 1994 and Burkert 1995 in dwarf galaxies, de Blok & McGaugh 1997 in LSB galaxies, Hernandez & Gilmore 1998 and Salucci 2001 for normal spirals, Tyson, Kochanski & Dell'Antonio 1998 for galaxy clusters). According to the analysis of rotation curves of dwarf and LSB galaxies carried out in Firmani et al. (2001), the core radius of the “virgin” halo of a galaxy of the size

of the MW should be  $\approx 10$  kpc with a central density of  $\approx 0.01 - 0.02 M_{\odot} \text{pc}^{-3}$ . To illustrate the effect that such a constant density core would have in terms of the rotation curve of the MW, we artificially smooth the inner density profile of the MW dark halo model along its evolution in such a way that at the present epoch it has such a core. The final rotation curve decomposition obtained after the formation of a MW disc in this halo is shown in Fig. 2a by the thin curves, which are analogous to the thick curves of the NFW case. The rotation curve is now almost completely flat and the disc component dominates over the halo component up to the solar radius, i.e., the dashed and dotted curves now intersect at approximately the solar radius, as direct studies of our galaxy show (e.g. Kuijken & Gilmore 1989). We can hence conclude that a comparison of dynamical studies in the MW and galactic evolutionary models offers yet another evidence of the excessive central concentration of CDM haloes predicted by the standard cosmology. Fortunately, the inclusion of a shallow core in the halo has no major consequences upon the SFH, as will be shown below.

#### 4 STAR FORMATION HISTORY IN THE SOLAR NEIGHBOURHOOD

As it is seen in Table 1, the properties of the MW fiducial model predict reasonably well the data inferred from observations, with the exception of the rotation curve. In Fig. 3a we show the evolution of the SFR per unit area and of the gas infall rate, both at the radius  $R_0 = 8.5$  kpc,  $\dot{\Sigma}_s(R_0, t)$  (solid line) and  $\dot{\Sigma}_g(R_0, t)$  (point-dashed line), respectively. The disc at the radius  $R_0$  begins to form at a look-back time  $\sim 11$  Gyr ( $z \approx 2$ ).

An interesting test derives from taking into account an integrated colour index for the solar neighbourhood. Using recent Padova stellar evolutionary models (e.g. Girardi et al. 1996) we computed synthetic colour magnitude diagrams for the average SFH, shown by the solid curve in Fig. 3a, taking a solar metallicity for the last 2 Gyr, and one third solar before this point, as a first approximation to the enrichment history. Calculating the  $B - K$  colour index for realizations containing upwards of 200,000 stars we obtain a value of  $B - K = 3.15$ , in excellent agreement with the solar neighbourhood observational estimate for this quantity of  $B - K = 3.13$  (Binney & Merrifield 1999). Repeating the experiment for SFHs resulting from MAHs deviating from the average one, we obtain practically identical values for the  $K$ -band luminosity, reflecting equal integrals under the SFH curves, but rather different values for the  $B$ -band luminosity, reflecting different recent SFHs. Taking the MAHs which differ most from the average (of the ones given in Fig. 1b), we obtain differences of 0.3 mag in the predicted  $B - K$  of the solar neighbourhood, rather larger than the observational uncertainties of the measured value. This important result leads us to expect the average MAH as the optimal choice for the Galaxy.

The recent observational inferences of Binney, Dehen & Bertelli (2000 henceforth DBD00) use kinematical data from the Hipparcos catalogue to break the age metallicity

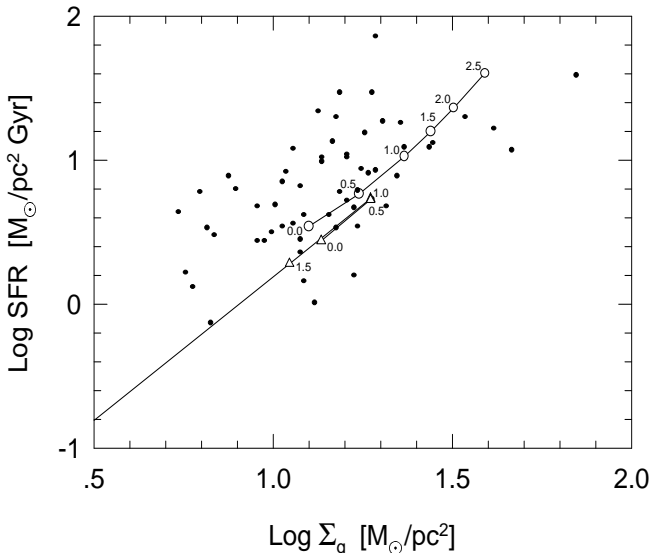


**Figure 4.** Evolution of the relation between surface SFR and surface gas densities, at the given redshifts, for the solar neighbourhood and the integrated Galaxy, jointed triangles and circles, respectively. A Schmidt law of power  $\approx 2$  is clearly seen as the final result of the SF physics we used. The solid dots show the data of Kennicutt (1998), corrected to take helium into account, for which a Schmidt law of power  $\sim 2$  is a good description.

ity degeneracy at the oldest turn off, identified also from the Hipparcos satellite by combining photometric data with theoretical isochrones. Their results for the age of the solar neighbourhood are shown by the shaded bar in Fig. 3a, and are clearly in good agreement with our predictions for the average MAH. The maximum rate of gas accretion at  $R_0$  is attained at  $\approx 10.5$  Gyr, and strongly decreases after this epoch. The SFH attains a broad maximum at 8–6 Gyr ( $z = 0.9 - 0.6$ ) and then smoothly declines by a factor of  $\approx 2$  towards the present day. The level of  $3.1 \text{ M}_\odot \text{pc}^{-2} \text{ Gyr}^{-1}$  we obtain for this quantity lies well within the range determined observationally, shown by the vertical shaded box at  $t=0$  Gyr (Talbot 1980, Rana 1987). A similar SFH is obtained for the MW model with a shallow core (thick dashed line), which illustrates the robustness of our results regarding SFHs, to the existing discrepancies in dark halo density profiles between theory and observations.

Our SFR at the solar radius is almost indistinguishable from an average of an annulus with inner and outer radii of 7.0 and 10 kpc, respectively. The local SFH inferred from observations might refer to an annulus of this size because due to stellar diffusion, stars which are today in the solar neighbourhood could have been formed at Galactocentric radii differing by up to  $\sim 1.5$  kpc (e.g. Dehnen & Binney 1998b).

The difference in shape between the SFH,  $\dot{\Sigma}_s(R_0, t)$ , and the gas infall history,  $\dot{\Sigma}_g(R_0, t)$ , depends on the turbulent dissipation time  $t_d$ ; the shorter  $t_d$  is, the closer  $\dot{\Sigma}_s(R_0, t)$  is to  $\dot{\Sigma}_g(R_0, t)$ . Nevertheless, the dissipation time we use is self-consistently calculated according to Firmani et al. (1996), and is in rough agreement with results from MHD numerical

simulations of the ISM (Avila-Reese & Vázquez-Semadeni 2001). We note that matching the constraints on the age of the solar neighbourhood of BDB00 with a different value of  $t_d$  would require the use of a MAH differing largely from the average one, a rather improbable situation.

In Fig. 3a we also show  $\dot{\Sigma}_s$  for the solar neighbourhood, as inferred recently by Bertelli & Nasi (2001), jointed circles. These authors used a volume-limited sample of field stars from the Hipparcos catalog and compared to synthetic color-magnitude diagrams generated for different parameter values of a SFH having a fixed parametric shape, and different stellar initial mass functions. Applying a  $\chi^2$  minimization, the best parameters of the *a priori* given SFH are found. In order to pass from the SFR per unit volume to the SFR per unit area, the total number of stars of age  $t$  found within the sampled sphere, as a fraction of the total over the disc height, a time dependent correction factor, must be known. This can be obtained with a procedure which takes into account the details of the vertical disc force law and the variations of velocity dispersion with age (e.g., Hernández et al. 2000b).

The SFH shown in Fig. 3a corresponds to the solution for the model with more degrees of freedom of the ones used in Bertelli & Nasi (2001) (their var-var model with  $I_b = 2$ ), and including the volume to surface density correction mentioned above. It must be noted that the detailed shape of the observed SFH is the result of the age dependent correction factor, as well as of the volume SFH solved for. As the authors emphasize, their method is useful to describe only the *general trend of the SFH over the total life of the system*, and not its detailed shape.

As it can be concluded from the  $\chi^2$  plots shown by these authors it is that the average SFR over the period 10–6 Gyr (in look-back time) could not have been larger than that over the 6–0 Gyr period. From Fig. 3a, this general trend is seen to agree well with the prediction of our fiducial model for the MW, suggesting that the main ingredients of the SF process in the MW were correctly taken into account, and that the MAH of the MW has been close to the average one.

The integration of the SFR in time gives the stellar surface density  $\Sigma_s$ , shown by the solid line in Fig. 3b, as a function of time, at  $R_0$ . The dashed line is the gas surface density  $\Sigma_g$ . At the present epoch,  $\Sigma_s(R_0) = 41.3 \text{ M}_\odot \text{pc}^{-2}$  and  $\Sigma_g(R_0) = 13.6 \text{ M}_\odot \text{pc}^{-2}$  in good agreement with observational measurements (Table 1). The evolution of the stellar surface density at the solar neighbourhood obtained with our model compares well to that derived by Fuchs et al. (2000) from a sample of G and K dwarfs with individually determined ages using their chromospheric HK emission fluxes, and assuming a given gas accretion history (see their Fig. 7).

Fig. 4 presents a global check of our SF mechanism. The open triangles show the time evolution of the solar neighbourhood in a log SFR vs.  $\log \Sigma_g$  plot, at  $z=0, 0.5, 1$  and  $1.5$ . The open circles show the temporal evolution for the whole modeled galaxy at  $z=0, 0.5, 1, 1.5, 2$  and  $2.5$ . The solid dots show the observations of normal galaxies by Kennicutt (1998) corrected to take helium into account. We have not included here the ULIRGs of that sample because they are

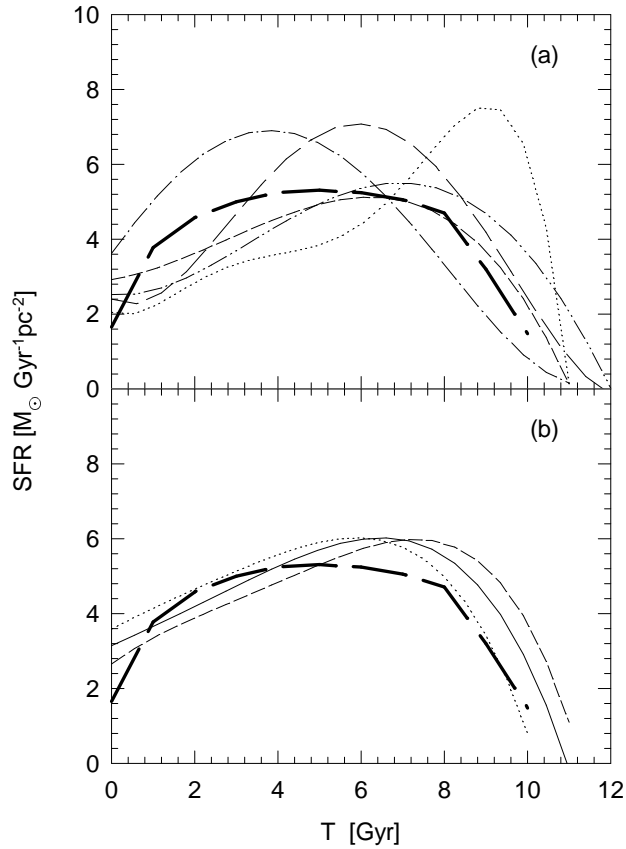


**Figure 5.** a) SHFs resulting from the five random MAHs of Fig. 1b, in matching line styles. The thick dashed curve shows the indicative results of Bertelli & Nasi (2001). b) Here we illustrate the variations in the predicted SFH of the solar neighbourhood as resulting from changing the input value of  $\lambda$  in consistency with the uncertainties in the observational determinations of the disc scale length, no strong dependence is seen. The thick dashed curve is the same as in panel a).

not representative of the SF regime of normal galaxies but are related to very strong SF bursts. In these cases, when the SFR exceeds the critical value  $\dot{\Sigma}_{s,c} = 300 M_{\odot} \text{pc}^{-2} \text{Gyr}^{-1}$  ( $\Sigma_{g,c} = 100 M_{\odot} \text{pc}^{-2}$ ) then SN energy injection no longer controls the SF, the control is transferred to the radiation pressure (Eddington limit). This duality in the SF self-regulation mechanism has been studied by Firmani & Tutukov (1994). For normal galaxies where the SFR is typically less than  $\dot{\Sigma}_{s,c}$  (the case of this work) self-regulation by SN energy injection leads to a Schmidt law of power  $\sim 2$ , while for the bursting SF regime with SFR greater than  $\dot{\Sigma}_{s,c}$  the self-regulation by radiation pressure leads to a Schmidt law of power  $\sim 1$ . The comparison of the open and filled symbols shows a rather satisfactory agreement indicative of a Schmidt law of power  $\sim 2$ . The slight offset of the data towards higher values of the SFR is not particularly meaningful because of the scatter of the observational data and the uncertainty on the turbulent dissipation time.

The shape of our resulting SFHs for the whole MW disc differ from that at the solar radius. The inside-out formation

of the disc and the mechanism of SF used here indeed lead to a differential evolution with radius of the galaxy (see also Boissier & Prantzos 1999, hereafter BP99), which highlights the importance of a dynamical galactic model in studies of galactic evolution where comparisons are made with spatially localized data.

#### 4.1 Sensitivity of the local SFH to the model input parameters

The input parameters of the MW evolutionary model presented above were chosen in such a way that the present-day properties obtained by the model agree with the observed structural parameters of the Galaxy,  $V_{50}$ ,  $r_s$  and  $M_s$  (see Table 1). Since the observational data are uncertain to some level and the model presents some degeneracy with respect to the input parameters, we need to explore the sensitivity of the predicted SFH in the solar neighbourhood to this input.

Due to the difficulty in determining the MAH for the MW from any observational constrain (see §3), we have taken the average MAH (fiducial model) as a first choice, as it represents the most probable cosmological solution for a MW mass galaxy. This obviously presents a smooth shape (Fig. 2a). However, other MAHs are also able to produce dark haloes consistent with the MW. In Fig. 1b we have five MAHs taken at random which, for a proper choice of the input parameters, can also give models in agreement with the main conditions we fixed for the MW. These MAHs are intrinsically discontinuous due to the stochastic nature of the primordial density fluctuation field. The SFHs at  $R_0 = 8.5$  kpc for the MW models produced with these MAHs are plotted in Fig. 5a, with the line style corresponding to the MAHs of Fig. 2a. We have included a smoothing on the results of these SFHs to facilitate the comparison with the results of Bertelli & Nasi (2001) (thick curve), as those results have a low time resolution.

As it can be seen, both the age of the solar neighbourhood and its present-day SFR are sensitive to the assumed MAH of the Galaxy. It is therefore these dependences that allows us to constrain the MAH of the MW. The observed age of the solar neighbourhood and its present SFR imply that the MAH of our Galaxy has been very close to the average one for present day objects of that mass.

The spin parameter  $\lambda$  is mainly constrained by the disc scale length  $r_s$ , which has an observational uncertainty of 1 kpc. In Fig. 5b we present the SFHs corresponding to MW models with the average MAH but with  $r_s = 2.5$  kpc (dotted line) and  $r_s = 3.5$  kpc (dashed line), the two extremes of the observational range. The difference in the SFHs is small. The more concentrated disc (smaller  $\lambda$ ) results in a later formation of the solar neighbourhood than the less concentrated one (larger  $\lambda$ ). The maximum in the SFH thus shifts slightly in time for these two alternative models, although much less than the changes resulting from varying the MAH. Therefore, uncertainties in the scale length do not alter our conclusions regarding the connection between the MAH and the SFH of the Galaxy.

Changes in  $f_d$  and  $M_v$  allowed by the uncertainties in  $V_{50}$  and  $M_s$  basically produce upward/downward shifts of

the local SFH directly proportional to  $M_s$ , the shape of the SFH remaining almost the same. No large variations of these parameters are possible, if we want the present day  $\Sigma_s$  and  $\Sigma_g$  at the solar neighbourhood to remain within the observed ranges.

Finally, we note that the Hubble parameter  $H_0$  plays a role in determining the cosmic time when the disc starts to form at the solar neighbourhood. The predicted SFH in the solar neighbourhood starts at lower look-back time when  $H_0$  is larger. For example, if we set  $H_0 = 80 \text{ km s}^{-1} \text{Mpc}^{-1}$ , then the disc at the solar neighbourhood forms at  $\approx 9.0$  Gyr, for the average MAH.

We find that the disc age at  $R_0$  for the fiducial model with  $H_0 = 65 \text{ km s}^{-1} \text{Mpc}^{-1}$  is consistent with observational estimates of the age of the solar neighbourhood (BDB00). Thus, the data offer a joint consistency check on the cosmological scenario, the galactic evolution model and the SF physics used.

## 5 DISCUSSION

### 5.1 Comparison with chemo-spectrophotometric models

In our approach, the local and global SF and infall gas histories of galaxies are predicted in a deductive way. In the case of models of chemical and spectrophotometric evolution, these histories are given in a parametric form and then constrained by comparing the model results with observations.

Much as the inversion of the high quality Hipparcos data allows for a reconstruction of the SFH of the solar neighbourhood, the large amount of observational constraints both for the solar neighborhood and over the whole disc allow the chemo-spectrophotometric models to constrict these histories (e.g., Prantzos & Aubert 1995; Chiappini et al. 1997; Prantzos & Silk 1998; BP99). However, most of the restrictions being time-integral constraints, the temporal resolution attained is low.

The SFHs in the solar neighborhood reported in Prantzos & Silk (1998) and in BP99 declines smoothly to the present epoch by a factor around two since its maximum, which is attained  $\sim 8 - 9$  Gyr and  $\sim 6 - 7$  Gyr ago, respectively. The main constraints for this smooth behaviour of the SFH, which agrees qualitatively with our prediction, are the observed differential metallicity distribution of long-lived G-dwarfs and the age-metallicity relation. These constraints also impose the necessity of a gradual gas infall, which again is in qualitative agreement with predictions of our model.

However, due to the phenomenological nature of the chemo-spectrophotometric models, a detailed reconstruction of the SFH is difficult to attain, in particular at early epochs. For example, in both papers, Prantzos & Silk (1998) and BP99, the solar neighborhood is assumed to form 13.5 Gyr ago, which is too early according to accurate kinematical and photometric studies (BDB00). Nevertheless, with an appropriate combination of the *a priori* gas infall history and SF law, the corresponding metallicity and surface density

constraints have been roughly satisfied in spite of the early formation of the solar neighborhood (degeneracy).

In as much as our results for global and local SFHs and gas infall rates do not deviate from those inferred by requiring consistency with the observational restrictions described above (BP99), we can expect our models to be also in agreement with the large variety of data regarding metallicities and abundance gradients in our Galaxy and for the solar neighbourhood.

### 5.2 Stationary and bursting star formation

Although we have assumed throughout that the main trends of the SF processes in the disc are well described by the stationary approach adopted, we are aware of the existence of ample evidence in favour of a more bursting character for this crucial ingredient, under some circumstances. However, as will be detailed below, we have reasons to believe that this alternative channel of SF will only introduce fluctuations of short temporal and spatial character, such that our stationary solution still represents the long term/large spatial trends accurately.

The method applied by Bertelli & Nasi (2001) allows a reconstruction of the broad trends in the local SFH over a long time interval ( $\sim 10$  Gyr), but it is not useful to trace fluctuations of short duration. The question of significant temporal fluctuations has been raised by Hernandez et al. (2000b) who in a direct and statistically grounded study of the colour magnitude diagram of Hipparcos find a modulation of a factor of  $\sim 1.5$ , with a period of  $\sim 0.5$  Gyr in the SFH of the solar neighbourhood. These authors interpret this as evidence of an enhancement of the SF activity caused by encounters with the spiral arm pattern density waves, a physical feature which is absent from our models. It is precisely the slowly oscillating character of the SFH found in that work, that justifies the interpretation of our results as the average over the inherent fluctuations of the Galactic SF process, i.e. this defines the temporal resolution of our present study to be of the order of 0.5 Gyr.

Even stronger time fluctuations in the SFH of the solar neighbourhood have been suggested by Rocha-Pinto et al. (2000), who argue against any steady (or self-regulated) component of the local SF. These authors use an empirical chromospheric activity indices vs. age relations to affix an age to each star in a sample of 552 late type dwarfs. However, the empirical relation used by these authors presents a strong scatter of around a factor 2 in age (their Fig. 22), which should be included as a time smoothing kernel on their final results. Interestingly, if such a smoothing is applied on their SFH, a trend similar to that reported in Bertelli & Nasi (2001) appears (see Fig. 8 in Rocha-Pinto et al. 2000). We therefore find the above study in fact strengthens any conclusions drawn from the work of Bertelli & Nasi (2001), from which no objections to the SF physics we are using are apparent.

A further mechanism responsible for strong time variations in the SF processes of galaxies is that of merger and tidally induced SF enhancements. However, this applies mostly to systems such as the strongly interacting galaxies

imaged by the *IRAS* satellite (Firmani & Tutukov 1994), or galaxies in dense cluster environments, see for a review Dultzin-Hacyan (1997). It is clear from the late type and low density environment of the MW that any alterations of the global SF due to interactions have been minor, and in all probability do not affect the conclusions of our study.

## 6 SUMMARY AND CONCLUSIONS

We have presented predictions of the SFH in the solar neighbourhood making use of a galactic evolutionary approach, tightly linked to a cosmological scenario. In this way we establish a direct connection between the evolution of the solar neighbourhood and the cosmological background. Within our deductive approach, galactic discs form inside out within growing CDM haloes. Star formation is triggered by disc gravitational instabilities and is self regulated by an energy balance in the turbulent ISM. In previous papers we have shown the ability of this approach to predict exponential discs over several disc scale lengths, as well as to reproduce the Tully-Fisher relation and several of the correlations across the disc Hubble sequence. Our results are also in qualitative agreement with the gas and SFR histories found to be consistent by comparing observations with chemo-spectrophotometric models.

The allowed MAHs for the MW result in SFHs for the solar neighbourhood which bracket the range of observational inferences. The average MAH for objects having the present day mass of the MW represents a cosmological maximum likelihood solution for the Galaxy. The SFH in the solar neighbourhood predicted for the above possibility, in the flat  $\Lambda$  CDM model used here, closely matches the available observational data.

For the cosmological galaxy evolution approach presented, the age of the solar neighbourhood as inferred from observations implies a delay in the conversion of the accreted gas into stars, consistent with our physical formulation of the SF process in disc galaxies.

For the value of  $H_0 = 65 \text{ km s}^{-1} \text{ Mpc}^{-1}$  used, the most probable MAH for our Galaxy implies an age for the solar neighbourhood of  $\approx 11$  Gyr, in agreement with direct observational inferences.

The rotation curve decomposition of the MW model is unrealistic if the disc forms within a CDM halo. If the halo has a shallow core of size and central density as inferred from rotation curves of dwarf and LSB galaxies, this problem is solved. Since the SFH is not affected by this, our conclusions regarding it and the cosmological build up processes of the Galaxy will remain for models where dark haloes present shallow cores.

## ACKNOWLEDGMENTS

The authors thank Liliana Hernández, Gilberto Zavala and Carmelo Guzmán for computing assistance. The work of V.A. was supported by CONACyT grants J33776-E and 27752-E.

## REFERENCES

Aparicio A., Bertelli G., Chiosi C., Garcia-Pelayo J.M., 1990, *A&A* 240, 262

Aparicio A., Gallart C., 1995, *AJ*, 110, 2105

Avila-Reese V., & Firmani C., 2000, *Rev. Mex. Astron. Astrofis.*, 36, 23 (AF00)

Avila-Reese V., & Firmani C., 2001, in "The VII Texas-Mexican Conference on Astrophysics: flows, blows, and glows", eds. W.H. Lee & S. Torres-Peimbert, *Rev. Mex. Astron. Astrofis. Serie de Conferencias*, vol. 10, 97

Avila-Reese V., & Vázquez-Semadeni E., 2000, *ApJ*, 553, 645

Avila-Reese V., Firmani C., & Hernández X., 1998, *ApJ*, 505, 37

Avila-Reese V., Firmani C., Klypin A., Kravtsov A., 1999, *MNRAS*, 310, 527

Baugh C.M., Cole S., Frenk C.S., 1996, *MNRAS*, 283, 1361

Bertelli G., & Nasi E., 2001, *AJ*, 121, 1013.

Binney J., Merrifield M., 1998, in "Galactic Astronomy" (Princeton University Press: New Jersey), p. 556

Binney J., Tremaine S., 1987, in "Galactic Dynamics" (Princeton University Press: New Jersey)

Binney J., Dehnen W., & Bertelli G., 2000, *MNRAS*, 318, 658

Buchalter A., Jiménez R., Kamionkowski M., 2001, *MNRAS*, 322, 43

Boissier S., & Prantzos N., 1999, *MNRAS*, 307, 857 (BP99)

Burles S., Nollett K.M., Truran J.N., Turner M.S., 1999, *Phys. Rev. Lett.*, 82, 4176

Burkert A., 1995, *ApJ*, 477, L25

Carigi L., 1996, *Rev. Mex. Astron. Astrofis.*, 32, 179

Catelan P., & Theuns T., 1996, *MNRAS*, 282, 436

Cen R., Ostriker J.P., 1999, *ApJ*, 519, L109

Chiapini C., Matteucci F., & Gratton R., 1997, *ApJ*, 477, 765

Chiosi C., Bertelli G., Meylan G., Ortolani S., 1989, *A&A*, 219, 167

Cole S., Aragón-Salamanca A., Frenk C.S., Navarro J., & Zepf S., 1994, *MNRAS*, 271, 781

Dalcanton J.J., Spergel D.N., Summers F.J., 1997, *ApJ*, 482, 659

Davé R., Cen R., Ostriker J.P., Bryan G.L., Hernquist L., Katz N., Weinberg D.H., Norman M.L., O'Shea B., 2000, *ApJ*, submitted (astro-ph/0007217)

de Blok W.J.G., & McGaugh S.S., 1997, *MNRAS*, 290, 533

Dehnen W., Binney J., 1998a, *MNRAS*, 294, 429

Dehnen W., Binney J., 1998b, *MNRAS*, 298, 387

Drimmel R., Spergel D.N., 2001, *ApJ*, in press (astro-ph/0101259)

Dultzin-Hacyan D., 1997, *Rev. Mex. Astron. Astrofis. Serie de Conferencias*, vol. 6, 132

Firmani C., Avila-Reese V., 2000, *MNRAS*, 315, 457 (FA00)

Firmani C., Tutukov A.V., 1992, *A&A*, 264, 37

Firmani C., Tutukov A.V., 1994, *A&A*, 288, 713

Firmani C., Avila-Reese V., Hernández, X., 1997, in "Dark and Visible Matter in Galaxies and Cosmological Implications", ed. M. Persic & P. Salucci, *ASP Conference Series* 117, 424

Firmani C., Hernández X., Gallagher J., 1996, *A&A*, 308, 403

Firmani C., D'Onghia E., Chincarini G., Hernández X., Avila-Reese V., 2000, *MNRAS*, 321, 713

Fich M., Tremaine S., 1991, *ARA&A*, 29, 409

Flores R., Primack J.R., 1994, *ApJ*, 427, L1

Fuchs B., Dettbarn C., Jahreis H., Wielen R., 2000, in *Dynamics of Star Clusters and the Milky Way*, ed. S. Deiters, B. Fuchs, A. Just, R. Spurzem, & R. Wielen, *ASP Conference Series*, in press

Fukushige T., Makino J., 1997, *ApJ*, 477, L9

Girardi L., Bressan A., Chiosi C., Bertelli G., Nasi E., 1996, *A&AS*, 104, 365

Haud U., Einasto J., 1989, *A&A*, 223, 95

Hernández X., Gilmore G., 1998, MNRAS, 294, 595  
 Hernández X., Valls-Gabaud D., & Gilmore G. 1999, MNRAS, 304, 705  
 Hernández X., Valls-Gabaud D., & Gilmore G. 2000a, MNRAS, 317, 831  
 Hernández X., Valls-Gabaud D., & Gilmore G. 2000b, MNRAS, 316, 605  
 Hernández X., Ferrara A., 2001, MNRAS, in press  
 Hogan C.J., 1998, Space Science Reviews, v. 84, 127  
 Kauffmann G., Charlot S., Balogh M.L. 2001, MNRAS, submitted (astro-ph/0103130)  
 Kauffmann G., White, S.D.M., & Guiderdoni, B. 1993, MNRAS, 264, 201  
 Kennicutt R.C. 1992, in Star Formation in Stellar Systems, ed. G. Tenorio-Tagle M. Prieto, & F. Sánchez (Cambridge Univ. Press), 191  
 Kennicutt R.C. 1998, ApJ, 498, 541  
 Kent S., Dame T., Fazio G., 1991, ApJ, 378, 131  
 Klypin A.A., Kravtsov A.V., Valenzuela O., Prada F., 1999, ApJ, 522, 82  
 Kochanek C.S., 1996, ApJ, 457, 228  
 Kuijken K., Gilmore G. 1989, MNRAS, 239, 571  
 Kulkarni S., Heiles C., 1987, in "Interstellar Processes", eds. D. Hollenbach & H. Thronson (Kluwer), 87  
 Lacey C.G., Cole S., 1993, MNRAS, 262, 627  
 Lacey C.G., Silk J. 1991, ApJ, 381, 14  
 Lilly S. et al., 1998, ApJ, 500, 75  
 Chiappini C., Matteucci F., Gratton R., 1997, ApJ, 477, 765  
 Mao S., Mo H.J., White S.D.M., 1998, MNRAS 296, 847  
 Madau P., Pozzetti L., Dickinson M., 1998, ApJ, 498, 106  
 McGaugh S. S., 1996, MNRAS, 280, 337  
 Méndez R.A., Platais I., Girard T.M., Kozhurina-Platais V., van Altena W.F., 1999, ApJ, L39  
 Mera D., Chabrier G., Schaeffer R., 1998, A&A, 330, 953  
 Michell K.J., Butcher H.R., 1992, A&A, 255, 26  
 Michell K.J., 1997, AJ, 114, 1458  
 Mo H.J., Mao S., White S.D.M., 1998, MNRAS, 295, 319  
 Mould J.R., Han M., Stetson P.B., 1997, ApJ, 483, L41  
 Moore, B. 1994, Nature, 370, 629  
 Moore, B., Ghigna, S., Governato, F., Lake, G., Quinn, T., Stadel, J., & Tozzi, P. 1999a, ApJ, 524, L19  
 Moore B., Quinn T., Governato F., Stadel J., Lake G., 1999b, MNRAS, 310, 1147  
 Navarro J., Benz W., 1991, ApJ, 380, 320  
 Navarro J., Steinmetz M., 2000, ApJ, 538, 477  
 Navarro J., Frenk C.S., White S.D.M., 1997, ApJ, 490, 493  
 Pagel B., 1997, in "Nucleosynthesis and Galactic Chemical Evolution" (Cambridge: Cambridge University Press, 1997)  
 Prantzos N., & Aubert, O. 1995, A&A, 302, 69  
 Prantzos N., & Silk, J. 1998, ApJ, 507, 229  
 Rana N., 1987, A&A, 184, 104  
 Rocha-Pinto H., & Maciel W. 1997, MNRAS, 325, 523  
 Rocha-Pinto H., Maciel W.J., Scalo J., & Flynn, C. 2000, A&A, 358, 869.  
 Sackett P.D., 1997, ApJ, 483, 103  
 Salucci P., 2001, MNRAS, 320, L1  
 Smecker-Hane T.A., Stetson P.B., Hesser J.E., Lehnert M.D., 1994 AJ, 108, 507  
 Somerville R.S., & Primack J.R. 1999, MNRAS, 310, 1087  
 Struck C., & Smith, D.C. 1999, ApJ, 527, 673  
 Talbot R.J., 1980, ApJ, 235, 821  
 Tolstoy E., Saha A., 1996, ApJ, 462, 672.  
 Tyson J., Kochanski G.P., & Dell'Antonio I. P., 1998 ApJ, 498, L107  
 van den Bosch F.C. 1998, ApJ, 507, 601  
 van der Kruit P., 1986, A&A, 157, 230  
 White S.D.M., & Frenk C.S. 1991, ApJ, 379, 52  
 Wilkinson M.I., Evans W., 1999, MNRAS, 310, 645